

See discussions, stats, and author profiles for this publication at: <https://www.researchgate.net/publication/27269839>

# Characterization and Structures of Dimeric C<sub>70</sub> Oxides, C<sub>140</sub>O, Synthesized with Hydrothermal Treatment

ARTICLE in THE JOURNAL OF PHYSICAL CHEMISTRY B · APRIL 2002

Impact Factor: 3.3 · DOI: 10.1021/jp0139989 · Source: OAI

CITATIONS

15

READS

19

8 AUTHORS, INCLUDING:



Balachandran Jeyadevan

The University of Shiga Prefecture

199 PUBLICATIONS 3,979 CITATIONS

SEE PROFILE



Kazuyuki Tohji

Tohoku University

341 PUBLICATIONS 6,188 CITATIONS

SEE PROFILE

# Characterization and Structures of Dimeric C<sub>70</sub> Oxides, C<sub>140</sub>O, Synthesized with Hydrothermal Treatment

Toshiji Kudo, Yuki Akimoto, Kozo Shinoda, Balachandran Jeyadevan, and Kazuyuki Tohji\*

Department of Geoscience and Technology, Tohoku University, Sendai, 980-8579, Japan

Takashi Nirasawa

Nihon Bruker Daltonics K.K., Tsukuba, 305-0051, Japan

Markus Waelchli

Bruker Biospin K.K., Tsukuba, 305-0051, Japan

Wolfgang Krätschmer

Max-Planck-Institut für Kernphysik, Postfach 103980, D-69029 Heidelberg, Germany

Received: October 30, 2001; In Final Form: February 4, 2002

The dimeric C<sub>70</sub> oxides were synthesized from C<sub>70</sub>/C<sub>70</sub>O mixed powder by hydrothermal treatment at 373 K for 12 h in aqueous NaOH solution. In this treatment, nucleophilic OH<sup>−</sup> ions are abundant and nucleophilic addition reactions were considered to synthesize dimeric fullerene oxides. The yield was estimated as ca. 2–3% summing up each isomer and also produced polyoxides, it is lower than that of C<sub>120</sub>O. Three isomers of C<sub>140</sub>O were isolated using High Performance Liquid Chromatography (HPLC) and characterized with UV–vis, FT-IR, and <sup>13</sup>C NMR and other methods. The results of these methods show a close similarity between C<sub>140</sub>O and C<sub>120</sub>O and support that our C<sub>140</sub>O samples exhibit the structure of conventional furan-bridged dimers. On the basis of the results of <sup>13</sup>C NMR and PM3 calculations, structure assignments for each sample were attempted.

## 1. Introduction

Fullerene oxides are one of the simplest fullerene derivatives and they indicate interesting reaction behavior during synthesis of dimeric species. The synthesis of the dimeric fullerene oxides such as C<sub>120</sub>O was stimulated by the discovery of the odd-numbered clusters C<sub>119</sub> in mass spectra of C<sub>60</sub>O<sup>1–3</sup> and Taylor's proposed mechanism for the generation of C<sub>119</sub> via thermal decarbonylation of C<sub>60</sub>O and addition of the resultant C<sub>59</sub> to C<sub>60</sub>.<sup>4</sup> In fact, C<sub>120</sub>O has also been synthesized with a mixture of C<sub>60</sub>/C<sub>60</sub>O<sup>5–7</sup> and Gromov et al. reported the production and characterization of C<sub>119</sub> synthesized from C<sub>120</sub>O in large quantities.<sup>8</sup> We also succeeded in the synthesis and isolation of dimeric fullerene oxides such as C<sub>120</sub>O and three isomers of C<sub>130</sub>O.<sup>9</sup> However, in the earlier reports, the synthesis of C<sub>140</sub>O using the C<sub>70</sub> oxides was not accomplished.<sup>10</sup> The reason for this was attributed to weak bonding between C<sub>70</sub> and the oxygen of C<sub>70</sub>O. Nevertheless, the presence of dimeric C<sub>70</sub> oxides in the MALDI-TOF mass spectra of C<sub>70</sub>O suggested the possibility of existence of C<sub>140</sub>O.<sup>11</sup> We believe that C<sub>140</sub>O could be synthesized in large quantities and may lead to the synthesis of C<sub>139</sub>. The less symmetrical C<sub>70</sub> is expected to yield less symmetrical dimers that have complicated structures but have interesting properties. In this work, we report the synthesis of dimeric C<sub>70</sub> oxides in large quantities using hydrothermal treatment of C<sub>70</sub>/C<sub>70</sub>O mixed powder in high pH water.<sup>9,10</sup> In the hydrothermal treatment, nucleophilic OH<sup>−</sup> ions are abundant and nucleophilic addition reaction stimulated the synthesis of

dimeric fullerene oxides as in C<sub>120</sub>.<sup>12</sup> At first, OH<sup>−</sup> ion attacks C<sub>70</sub>O and yields intermediate C<sub>70</sub>OHO<sup>−</sup>. Then C<sub>70</sub>OHO<sup>−</sup> reacts with neighboring C<sub>70</sub> to form (C<sub>70</sub>OHO–C<sub>70</sub>)<sup>−</sup>. After electron transfers within (C<sub>70</sub>OHO–C<sub>70</sub>)<sup>−</sup>, finally C<sub>140</sub>O is formed releasing OH<sup>−</sup> ion. Detailed formation mechanism of dimeric fullerene oxides in hydrothermal treatment is described in ref 9. Hydrothermal treatment can also synthesize water-soluble fullerenes that are believed to be poly-hydroxylated fullerenes, in the case that highly oxidized fullerenes are used as starting material. In this experiment too, water-soluble C<sub>70</sub> might be synthesized; however, the solution containing the species was removed at the stage of hydrothermal treatment and was not considered for further analysis. Detailed information about the synthesis of water-soluble fullerenes is described elsewhere.<sup>13</sup> Furthermore, we succeeded in isolating three isomers of C<sub>140</sub>O that were characterized and investigated with several spectroscopic methods.

## 2. Experiment

### 2–1. Synthesis and Isolation of Dimeric C<sub>70</sub> Oxides.

The fullerene C<sub>70</sub> used in this experiment was extracted and isolated from the fullerene soot synthesized by the arc discharge method using a Soxhlet extractor and HPLC with a Buckyprep column (with a diameter of 20 mm and a length of 250 mm, Nakarai Tesque Co. LTD, Japan) for separation. The purity of the starting material C<sub>70</sub> was higher than 99%. Then, C<sub>70</sub> was oxidized by dissolving in toluene and bubbling with ozone. C<sub>70</sub>/C<sub>70</sub>O powder was produced by pouring the C<sub>70</sub>/C<sub>70</sub>O toluene solution into methanol. Later, dimeric C<sub>70</sub> oxides were synthe-

\* To whom correspondence should be addressed.

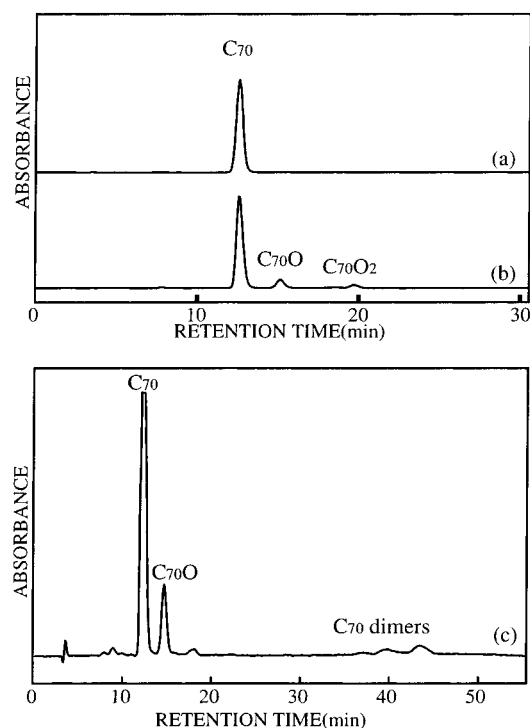


**Figure 1.** HPLC charts of toluene solution of (a) starting  $C_{70}$ , (b)  $C_{70}$  after ozone bubbling, and (c)  $C_{70}/C_{70}O$  mixture after hydrothermal treatment (Cosmosil Buckyprep column, toluene elution, 330 nm detection).

sized through nucleophilic addition reaction by heating the powder at 373 K for 12 hours in an aqueous NaOH solution of pH 13 or higher. After HPLC analysis with a Buckyprep column (diameter of 4.5 mm and a length of 250 mm) and mass analysis, the product was dissolved in toluene, and a rough separation of dimeric  $C_{70}$  oxides from  $C_{70}/C_{70}O$  and the isolation of three isomers of  $C_{140}O$  were carried out.

## 2-2. Characterization.

Matrix-Assisted Laser Desorption/Ionization Time-Of-Flight (MALDI-TOF) mass spectra of each sample were measured with a pulsed  $N_2$  laser (337 nm) using 9-nitroanthracene as a matrix (REFLEX III model of Bruker Co. Ltd., Germany). Absorption spectra were measured using a UV-vis spectrophotometer (U-3300 of HITACHI Co. Ltd.). Infrared absorption (IR) spectra were obtained from powder sample embedded in KBr pellets using FT-200 (HORIBA Co.) with resolution of  $4\text{ cm}^{-1}$ . Raman spectra were obtained by dropping the sample dissolved in ODCB solutions on brass target and evaporating the solvent. The spectrometer was of type T64000 (Dilor-Jobin Yvon-Spex Co.) with a 514.5-nm wavelength Ar ion laser (Leonix Co.). Finally,  $^{13}\text{C}$  NMR spectra were obtained at 125.76 MHz with Cryoprobe DRX500 FT-NMR spectrometer of Bruker. For the measurement, 0.4 mL of saturated solutions (ODCB- $d_4$ ) of  $C_{140}O$  isomers were prepared in a 5-mm NMR tube with ca. 16 mM  $\text{Cr}(\text{acac})_3$  for paramagnetic relaxation enhancement. Although these samples were not enhanced with  $^{13}\text{C}$ , we succeeded in acquiring good spectra with Bruker Cryoprobe. Normal acquisition, resolution enhanced, and spin-echo spectra were used for the identification of the peaks.

## 3. Results

### 3-1. Synthesis and Isolation.

Figure 1 a and b show the HPLC charts of  $C_{70}$  and  $C_{70}/C_{70}O_n$  ( $n > 2$ ) synthesized by ozone bubbling, respectively. New peaks were recorded showing the existence of  $C_{70}$  oxides.  $C_{140}O$  was

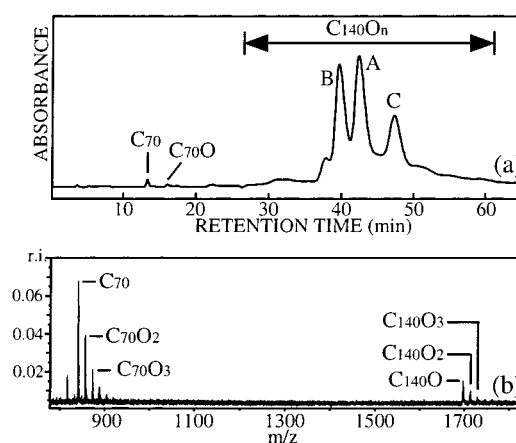
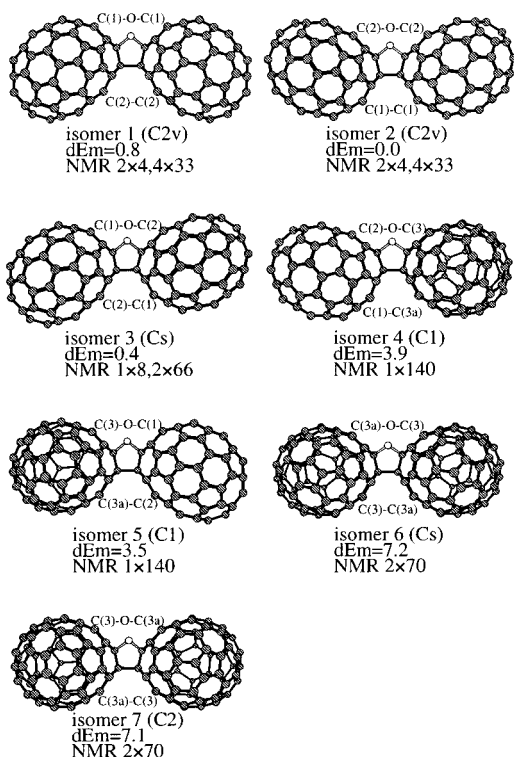


**Figure 2.** HPLC chart and MALDI-TOF mass spectrum (9-nitroanthracene was used as a matrix) of roughly separated dimeric  $C_{70}$  oxides. Relative intensities between monomeric species and dimeric species are different between HPLC chart and mass spectrum. This is caused by fragmentation of  $C_{140}O$  in mass spectrometer. HPLC chart shows more reliable data for quantitative analysis.

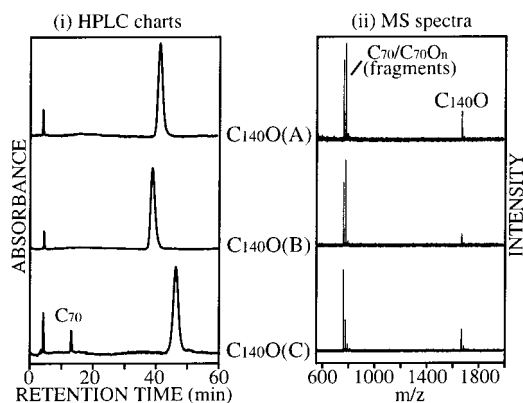
synthesized using the obtained  $C_{70}/C_{70}O_n$  as the starting material. Figure 1c shows the HPLC chart of the substance resulting from hydrothermal treatment. Though the intensities were small, new peaks with long retention time were recorded. The intensities of these new peaks were very low and close to the detectable limit of our HPLC apparatus. Therefore, under the hypothesis that these peaks originate from dimeric  $C_{70}$  oxides and their isomers, this region was roughly separated from  $C_{70}/C_{70}O_n$  monomer species using HPLC. Then, the sample was evaporated and analyzed using HPLC and MALDI-TOF-MS (Figure 2).  $C_{140}O$  has been predicted to have seven isomers by Fowler et al. (Figure 3),<sup>14</sup> and the HPLC analysis showed several peaks suggesting the presence of isomers. On the other hand, not only the presence of  $C_{140}O$  but also  $C_{140}O_2$  or higher oxides were inferred from the MS analysis of the sample. From these experimental results and the theoretical prediction, this region was believed to include many isomers and polyoxides of  $C_{140}O$ , for example,  $C_{140}O_2$ . To examine these polyoxides, we attempted to synthesize  $C_{140}O$  from material free of  $C_{70}O_2$  prepared using HPLC. Nevertheless, the resulting substance did not show any difference, suggesting nonparticipation of  $C_{70}O_2$  in the reaction. We believe that this was due to the low stability of  $C_{70}O_2$ . With the thermal energy acquired during the experiment,  $C_{70}O_2$  could easily dissociate to  $C_{70}O$  or  $C_{70}$  by releasing oxygen atom. The yield of dimeric  $C_{70}$  oxides was estimated as ca. 2–3% summing up the peak area represented by each isomer and polyoxides in the HPLC profile. We believe that the low yield and long retention time prevented the discovery of  $C_{140}O$  in the earlier studies.<sup>10</sup>

Figure 4i shows HPLC charts of isolated isomers of  $C_{140}O$  marked with A–C in Figure 2. In this figure, HPLC charts of  $C_{140}O$ (A) and (B) do not show any difference except for their respective retention times. On the other hand, the peak of  $C_{70}$  was recorded only in the chart of  $C_{140}O$ (C). To remove this peak, we repeated HPLC separation for  $C_{140}O$ (C); however, complete removal of the same was impossible. From the above results, we believe that  $C_{140}O$ (C) is an unstable isomer in comparison to A or B. Then,  $C_{140}O$ (C) was believed to have dissociated in the process of HPLC separation or during evaporation after HPLC.

Figure 4ii shows MALDI-TOF mass spectra of isolated isomers of  $C_{140}O$ . Similar to the HPLC result, there was no remarkable difference between mass spectra of  $C_{140}O$ (A)



**Figure 3.** Seven isomers of C<sub>140</sub>O with their individual symmetry. dEm means relative energy in kJ mol<sup>-1</sup> calculated with the MNDO model by Fowler et al., and the reliable <sup>13</sup>C NMR patterns of intensities are shown. As for the numbering of carbon atoms in C<sub>70</sub> [C(1)–O–C(1), C(2)–C(2), etc.], refer to Figure 10.



**Figure 4.** HPLC charts and MALDI-TOF mass spectra of isolated isomers of C<sub>140</sub>O.

and(B); however, mass spectrum of C<sub>140</sub>O(C) showed less intense mass peak of C<sub>70</sub>O and more intense mass peaks of polyoxides of C<sub>70</sub>O and C<sub>140</sub>O in comparison to that of C<sub>140</sub>O(A) and (B). From these results, we conclude that the oxygen atom in C<sub>140</sub>O(C) easily dissociates and attaches to an adjacent molecule compared to C<sub>140</sub>O(A) and (B).

### 3–2. Electronic Absorption.

The UV–vis absorption spectra of each of the isomers of C<sub>140</sub>O were similar to that of C<sub>70</sub>, but the bands are broadened and shifted. These differences may result from the less symmetrical structure of C<sub>140</sub>O. The onset seemed to be at slightly longer wavelength compared to C<sub>70</sub>. In C<sub>140</sub>,<sup>15</sup> the HOMO–LUMO gap has been ascertained both theoretically and experimentally to be smaller than C<sub>70</sub>. C<sub>140</sub>O could also be expected to have smaller HOMO–LUMO gap compared to C<sub>70</sub>. Typical tendencies were also observed in the spectra of other dimeric fullerene oxides such as C<sub>120</sub>O and C<sub>130</sub>O.

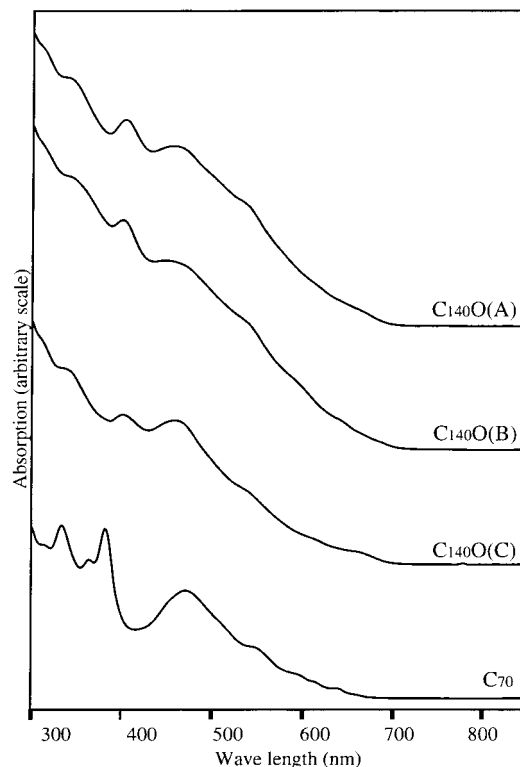


**Figure 5.** UV–vis absorption spectra of isolated isomers of C<sub>140</sub>O (upper three spectra) and C<sub>70</sub> (bottom).

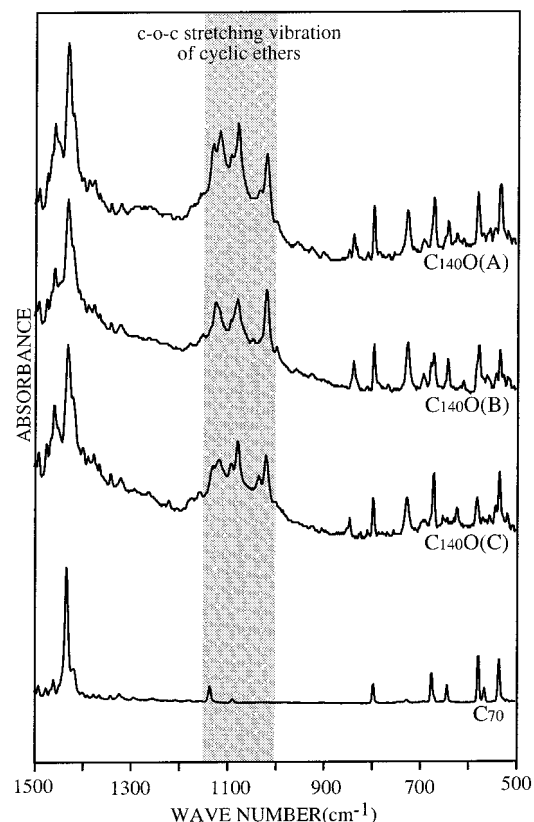


**Figure 6.** FT-IR absorption spectra of isolated isomers of C<sub>140</sub>O (upper three spectra) and C<sub>70</sub> (bottom).

### 3–3. Vibrational Spectroscopy.

Figure 6 shows FT-IR spectra of isolated isomers of C<sub>140</sub>O. Each isomer showed peaks similar to that of C<sub>70</sub>; however, they were shifted and split. This is caused by the reduced symmetry

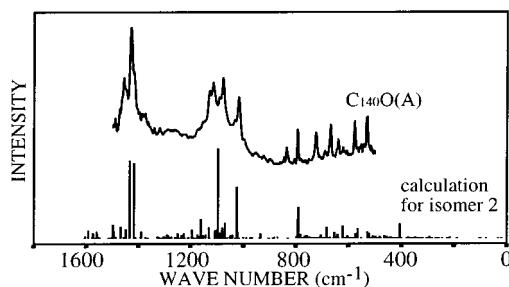


**Figure 7.** Calculated IR spectrum of  $C_{140}O$  isomer 2 and experimental FT-IR spectrum of  $C_{140}O(A)$ .

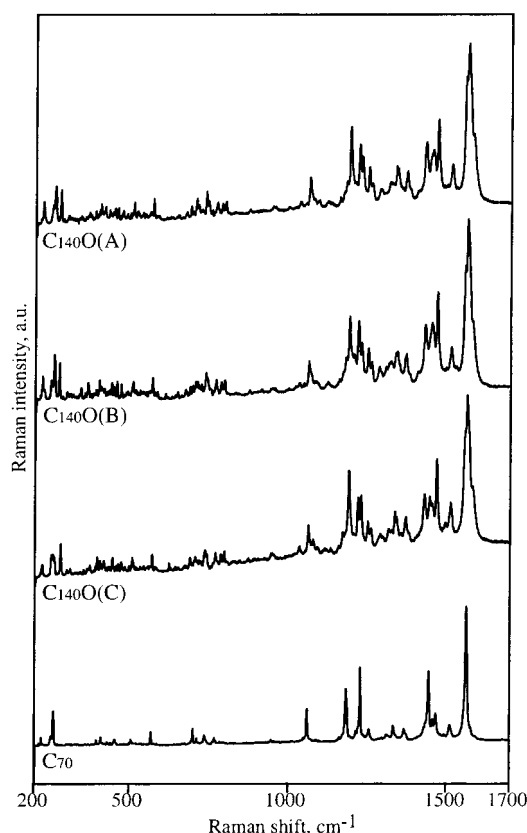


**Figure 8.** Raman spectra obtained by Ar ion laser excitation at 514.5 nm from isolated isomers of  $C_{140}O$  (upper three spectra) and  $C_{70}$  (bottom).

and perhaps the interaction between the two  $C_{70}$  cages. The most remarkable difference between the isomers of  $C_{140}O$  and  $C_{70}$  is the existence of peaks in the range from 1000 to 1150  $cm^{-1}$ . Peaks in this range were considered to represent C–O–C vibration of dimeric fullerene oxide and were also observed in the IR spectra of  $C_{120}O$  and  $C_{130}O$ .<sup>5,9,10</sup> This result suggested that  $C_{140}O(A)$ , (B), and (C) have the structure of conventional dimeric fullerene oxides, which are furan-bridged. The theoretical IR spectrum for  $C_{140}O$  isomer 2 calculated with Hyperchem is shown in Figure 7 and exhibits a good agreement with experimental spectrum. In this theoretical spectrum, there are roughly three groups of lines: groups at around 600, 1100, and 1400  $cm^{-1}$ . The group at 1100  $cm^{-1}$  basically corresponds to C–O–C stretching modes of the furan connection between the  $C_{70}$  balls. The others are C–C modes within the  $C_{70}$  units. The group at around 600  $cm^{-1}$  corresponds to radial motions, and the one at around 1100  $cm^{-1}$  corresponds to the motions on the  $C_{70}$  surface. This calculation should also support the furan-bridged structure of  $C_{140}O$  samples. Furthermore, the peak profile of  $C_{140}O(B)$  in this C–O–C range seemed different from

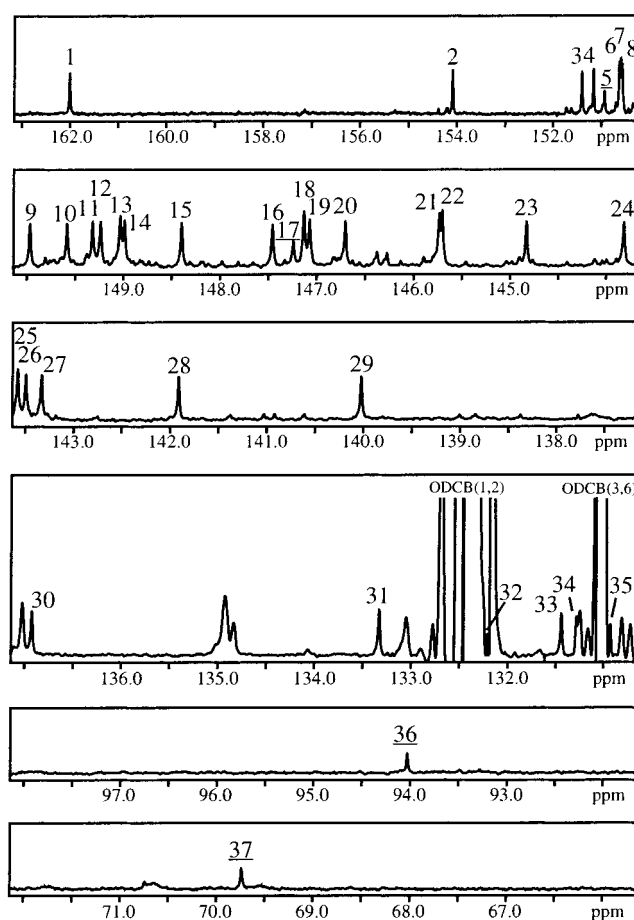


**Figure 9.** 125.76 MHz  $^{13}C$  NMR spectrum of  $C_{140}O(A)$  in *o*-dichlorobenzene- $d_4$  with  $Cr(acac)_3$  for paramagnetic relaxation enhancement. This sample was not enriched in  $^{13}C$ . This spectrum was obtained with normal acquisition without 1H decoupling. Repetition time was 3 s and experimental time was 24 h. Peak assignment was done by comparing this spectrum and spin-echo spectrum.

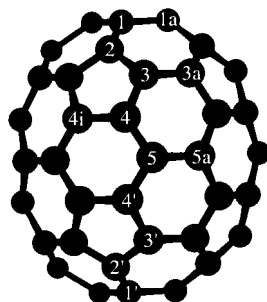
that of  $C_{140}O(A)$  and (C). This should be related to different C–O–C vibration modes in each isomer, caused by different junctions between two  $C_{70}$  cages. This may be used for the structure assignment of each isomer and will be discussed in section 4–1. In addition, split peaks of each isomer in the range of small wavenumber (500–1000  $cm^{-1}$ ) were different from each other. It is well known that IR spectra are related to the structure or the symmetry of substance. Therefore, these differences suggested that the structure of each sample was different.

Figure 8 shows Raman spectra of isolated isomers of  $C_{140}O$ . Showing a similar trend with FT-IR, peaks of  $C_{140}O$  isomers in Raman spectra were shifted and split compared to that of  $C_{70}$ . In each spectrum, there were slight differences in the relative intensities of each peak, but not as large as observed in FT-IR spectra. In dimeric fullerene species, it was reported that new peaks related to intercage vibration modes<sup>15–20</sup> were observed in the region around 100  $cm^{-1}$ . Therefore, the existence of peaks in this region could support the dimeric structure of our samples. However, we could not obtain reliable data because of bright lines of the Ar ion laser.

### 3–4. NMR Measurements.

The  $^{13}C$  NMR spectrum of  $C_{140}O(A)$  is shown in Figure 9, and assigned resonances (37 peaks) are numbered and listed in Table 1. This spectrum corresponded to a single isomer of  $C_{140}O$ . The presence of other dimeric species as impurities was discarded because of the absence of any peaks in the  $sp^3$  region





**Figure 10.** Structure of C<sub>70</sub> with labeling to show the reaction site. The numbering is used to define the longitude and the letters a, b, c, etc. are used to define the latitude moving from west to east. Among eight possible reaction sites (1–1a, 1–2, 2–3, 3–3a, 3–4, 4–4i, 4–5, and 5–5a), the sites that have “formal double bond” are only 1–2 and 3–3a. 1–2 is called “polar” and 3–3a is called “tropical”.

**TABLE 1:** <sup>13</sup>C NMR Data for C<sub>140</sub>O(A) in ODCB-d<sub>4</sub>

no.	ppm	integral	no.	ppm	integral
1	162.32	4.00	20	147.03	4.04
2	154.4	3.92	21	146.06	4.32
3	151.71	3.88	22	146.03	4.76
4	151.47	4.12	23	145.16	3.96
5	151.25	1.92	24	144.14	4.56
6	150.94	4.60	25	143.92	4.68
7	150.91	3.88	26	143.83	4.68
8	150.91	4.44	27	143.67	4.68
9	150.29	3.92	28	142.25	3.84
10	149.91	4.08	29	140.36	4.04
11	149.7	4.44	30	137.26	4.20
12	149.56	4.64	31	133.66	4.08
13	149.36	5.00	32	132.54	0.76
14	149.31	4.20	33	131.77	3.44
15	148.72	4.20	34	131.61	2.40
16	147.78	3.84	35	131.26	1.52
17	147.57	2.52	36	94.36	1.60
18	147.46	5.68	37	70.07	1.88
19	147.4	4.84			

of the spectrum except of the two peaks originated from C<sub>140</sub>O(A). The numbers of NMR peaks for isomers 1 and 2 were predicted to be 37 by Fowler et al. (Figure 3).<sup>14</sup> Therefore, C<sub>140</sub>O(A) was considered to be either isomer 1 or 2. The only difference between isomer 1 and 2 is the position of the oxygen atom. In isomer 1 and 2, the oxygen atoms are attached to carbon atom no. 1 and 2, respectively, as shown in Figure 10.

Figure 11 shows the <sup>13</sup>C NMR spectrum of C<sub>140</sub>O(B), and 139 NMR peaks are numbered and listed in Table 2. Large solvent peaks are considered to hide one of 140 peaks. The peaks of one major isomer and minor isomer(s) were found from the spectrum. From the peak integrals, concentration of the minor

**TABLE 2:** <sup>13</sup>C NMR Data for C<sub>140</sub>O(B) in ODCB-d<sub>4</sub>

ppm	I	ppm	I	ppm	I
162.90	1	148.21	1	144.26	1
161.96	1	148.15	1	144.23	1
157.46	1	147.80	1	144.06	1
155.65	1	147.74	3	143.96	1
154.84	1	147.61	1	143.91	1
154.47	1	147.58	3	143.89	1
154.16	1	147.53	2	143.83	1
152.03	1	147.47	1	143.74	1
152.01	1	147.42	1	143.35	1
151.85	1	147.27	2	142.66	1
151.62	3	147.22	1	142.24	1
151.39	1	147.14	1	142.01	1
151.06	3	147.11	1	141.82	1
150.96	1	146.92	1	141.16	1
150.89	1	146.83	1	140.66	1
150.75	1	146.78	1	140.31	1
150.69	1	146.67	1	137.20	1
150.36	1	146.52	1	137.13	1
150.20	2	146.38	1	133.86	1
150.10	1	146.33	1	133.66	1
150.02	1	146.27	2	132.37	1
150.00	1	146.21	1	132.00	1
149.91	1	146.19	1	131.77	1
149.80	1	146.16	1	131.75	1
149.78	1	146.07	1	131.65	1
149.74	1	146.04	2	131.53	1
149.73	1	145.93	1	131.38	1
149.66	1	145.45	1	131.34	1
149.58	1	145.44	1	131.15	1
149.50	1	145.27	1	130.94	1
149.45	3	145.18	1	130.99	1
149.41	1	145.16	1	130.14	1
149.36	1	144.94	1	130.09	1
149.33	1	144.78	1	126.96	1
150.31	1	144.69	2	125.83	1
149.28	1	144.53	1	94.79	1
149.23	1	144.48	1	90.59	1
148.88	1	144.44	1	72.95	1
148.82	3	144.38	1	67.99	1
148.58	1	144.36	1		
148.34	1	145.29	1		

isomer was estimated to be 10–15%, but it was impossible to count the number of peaks as most of them were hidden in the major peaks. In the theoretical prediction by Fowler et al., isomers that have 140 peaks were isomers 4 and 5. Similar to isomer 1 and 2, the only difference between isomers 4 and 5 was the position of oxygen atom.

Unfortunately, the S/N ratio of <sup>13</sup>C NMR spectrum of C<sub>140</sub>O(C) was not high enough to count the number of peaks. This was due to low stability of C<sub>140</sub>O(C), which precipitated in a few hours at the concentration necessary for NMR measurements. Nevertheless, we found that C<sub>140</sub>O(C) has at least 60 NMR peaks.

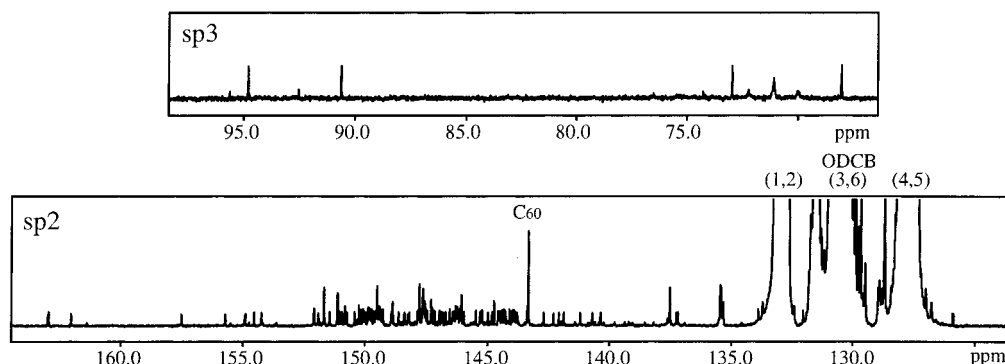


**Figure 11.** 125.76 MHz <sup>13</sup>C NMR spectrum of C<sub>140</sub>O(B) in o-dichlorobenzene-d<sub>4</sub> with Cr(acac)<sub>3</sub> for paramagnetic relaxation enhancement. Also, this sample was not enriched in <sup>13</sup>C. Repetition time was 3 s and experimental time was 56 h. Large peak at 143.29 ppm is attributed to C<sub>60</sub> as contaminant.

## 4. Discussion

### 4-1. Structure of C<sub>140</sub>O.

Theory predicts that C<sub>140</sub>O should have seven isomers (Figure 3). The formal double bonds in C<sub>70</sub> are limited to its capping region and are classified into "polar" double bonds and "tropical" double bonds named in ref 14. The former radiates from the pentagon of the 5-fold axis, and the latter links the circuit of five pentagons. From the combination of these two formal double bonds, the alternative direction of C<sub>70</sub> and the position of the oxygen atom, seven isomers are possible.

From the NMR measurements, it was clear that C<sub>140</sub>O(A) should have the structure of isomer 1 or 2. Since isomer 1 and 2 have the same C<sub>2v</sub> symmetry, it was difficult to distinguish one from the other even with Raman or IR spectra as much as NMR spectra. According to the MNDO calculation by Fowler et al., isomer 2 has a more favorable structure (see Figure 3; dEm (isomer 1) = 0.8, dEm (isomer 2) = 0.0). Energetically, the difference between them is marginal and it is risky to determine the structure only from theoretical calculations. Further, the theoretical calculation cannot explain the reason for the synthesis of only one of the isomers 1 or 2 (or 4 or 5) in large quantity. By the way, Lebedkin et al.<sup>15</sup> has already succeeded in the synthesis, isolation, and structural determination of dimeric C<sub>70</sub>, that is, C<sub>140</sub>. They also considered two structures from the result of NMR measurements. Nevertheless, they succeeded in the structural determination from the well-known structure of C<sub>70</sub> crystal. In our case, structural determination was very difficult as there is no structural information on C<sub>70</sub>/C<sub>70</sub>O<sub>n</sub> mixed crystals available.

Here, we propose the possible structural assignment based on the position of the oxygen atom in C<sub>140</sub>O. As a matter of fact, C<sub>70</sub>O is needed for the synthesis of C<sub>140</sub>O. Only two types of C<sub>70</sub>O can be synthesized with almost equal yield.<sup>21-23</sup> One of them is of (1,2) type and the other is of (3,3a) type (see Figure 10). According to several theoretical calculations,<sup>24,25</sup> the most stable isomer of C<sub>70</sub>O is (5,5a) type, though the reason is unclear. The (1,2) and (3,3a) type isomers are produced during synthesis. For the synthesis of C<sub>140</sub>O, one of two C–O bonds in C<sub>70</sub>O should be broken. But in the case of (3,3a) type, these two bonds are symmetrical and equivalent to each other. Thus, the selectivity of the breaking bond does not affect the subsequent structure of C<sub>140</sub>O. On the other hand, the (1,2) type also has two C–O bonds; however, they are not equivalent. In our semiempirical PM3 calculations using CS MOPAC software equipped in CS ChemBats3D Pro, the bond lengths do not show a clear difference (0.1424 nm for C(1)–O bond and 0.1425 nm for C(2)–O bond). However, the Mulliken charges are different, 0.08485e for C(1) and 0.07571e for C(2). Also in other calculation methods such as AM1 and MNDO, the charge of C(1) is higher than that of C(2) though the absolute values are different from the PM3 method. In the synthesis of dimeric fullerene oxides through hydrothermal treatment, the formation of dimeric fullerene oxides has been proposed through the nucleophilic addition reaction. As it is well known, nucleophile (in our case, OH<sup>−</sup> ions) attacks preferentially the positively charged portion of the molecule in the above reaction. Therefore, we believe that OH<sup>−</sup> ion tends to attack the C(1) atom, which has higher charge, and to break the C(1)–O bond rather than the C(2)–O bond. Taking this into account, we propose that C<sub>140</sub>O(A) contains the structure of isomer 2.

Also for C<sub>140</sub>O(B), two structures were considered from NMR measurements. Complete structural assignment was impossible for the same reason as in C<sub>140</sub>O(A). Nevertheless, we suppose that the structure of C<sub>140</sub>O(B) corresponds to isomer 4 for the

reason mentioned above. However, this assignment does not match with the energetic calculation by Fowler et al.<sup>14</sup> The energetic difference between isomer 4 (dEm = 3.9) and isomer 5 (dEm = 3.5) is marginal. Isomer 4 and 5 could be formed from (3,3a) type C<sub>70</sub>O that has symmetrical C–O bonds. Therefore, on the basis of simple calculation, the ratio of yields between isomers 4 and 5 should be 3:1. This calculation is under the hypothesis that equal amounts of (1,2) type C<sub>70</sub>O and (3,3a) type C<sub>70</sub>O are included in the starting material, (1,2) type C<sub>70</sub>O yields isomer 4 only, and (3,3a) type C<sub>70</sub>O yields both isomer 4 and 5 in equal efficiency. In this study, only the species marked with A, B, and C in Figure 2 were isolated and investigated. It thus appears that isomer 5 was not found; however, we believe that it should exist in the sample after hydrothermal treatment.

Unfortunately, the <sup>13</sup>C NMR spectrum of C<sub>140</sub>O(C) could not be obtained with high S/N ratio. Therefore, perfect structural determination of C<sub>140</sub>O(C) was impossible. However, we can propose the structure by interpreting FT-IR spectra. In the C–O–C vibration region, C<sub>140</sub>O(A) and (C) have similar profiles with three major peaks and three minor peaks, but C<sub>140</sub>O(B) was different and free of minor peaks. These differences were considered because of the difference in the junction between two C<sub>70</sub> cages. In C<sub>140</sub>O(A), namely, isomer 2 (or 1), the junction can be described as (1,2)/(1,2) [or (2,1)/(2,1)]. On the other hand, in C<sub>140</sub>O(B) (isomer 4 or 5), the junction can be described as (1,2)/(3,3a) or (2,1)/(3,3a). Therefore, the split of peaks in C<sub>140</sub>O(A) and (C) in the C–O–C vibration region could be attributed to the junction at the (1,2) site in C<sub>70</sub>. These types of junction have relatively higher symmetry. Among all seven isomers, the ones that have the above junction were isomers 1, 2, and 3. The number of NMR peaks for both isomer 1 and 2 is 37. As mentioned above, at least 60 NMR peaks were found in the spectrum of C<sub>140</sub>O(C). This suggests that C<sub>140</sub>O(C) could not have the structure of isomer 1 or 2. From this elimination method, we believe that C<sub>140</sub>O(C) has the structure of isomer 3. This unstable isomer was predicted to be relatively stable in the theoretical calculation by Fowler et al.<sup>14</sup> Unfortunately, we cannot provide a clear interpretation for this discrepancy, but the predictions of Fowler et al. for various dimeric fullerene oxide species were usually confirmed by experiment.

In summary, the <sup>13</sup>C NMR measurements provides firm evidence that (1) C<sub>140</sub>O(A) corresponds to the structure of isomer 1 or 2 and (2) C<sub>140</sub>O(B) corresponds to the structure of isomer 4 or 5. On the other hand, from PM3 calculation for Mulliken charge distribution and from FT-IR measurements, we concluded that C<sub>140</sub>O(A) and (B) correspond to the structure of isomers 2 and 4, respectively. Furthermore, C<sub>140</sub>O(C) has the structure of isomer 3.

### 4-2. Alternative Method for the Synthesis of C<sub>140</sub>O.

In this paper, we used the hydrothermal treatment for the synthesis of dimeric fullerene oxides. However, several other methods have been already reported for the synthesis of dimeric fullerene oxides.<sup>5,7</sup> Among them, we attempted Lebedkin's method where C<sub>60</sub>/C<sub>60</sub>O mixed powder is heated to 473 K in an Ar atmosphere.<sup>5</sup> At first, the C<sub>70</sub>/C<sub>70</sub>O<sub>n</sub> starting material was heated to 473 K under similar experimental condition as in the case of C<sub>120</sub>O. From the resulting substance, HPLC and mass peaks of C<sub>140</sub>O were observed. However, a large part of substance was insoluble in both toluene and o-dichlorobenzene. Mass analysis suggested the substance to be polymeric C<sub>70</sub> oxides, and the reaction temperature of 473 K was considered to be too high for C<sub>70</sub> species. From the analysis of the products

synthesized at various temperatures, the optimum temperature for the synthesis of C<sub>140</sub>O was considered to be 423 K. Though the yield of C<sub>140</sub>O synthesized under this condition was slightly higher than the hydrothermal method, the yield of insoluble species was comparatively high. C<sub>70</sub> is not so an abundant fullerene as C<sub>60</sub> and also, the efficient conversion of polymeric fullerene oxide species to its monomer is not known to date. Therefore, we believe that our hydrothermal treatment is the most suitable method for the synthesis of C<sub>140</sub>O from the viewpoint of recycling unreacted C<sub>70</sub>.

## 5. Summary

We have shown that C<sub>140</sub>O could be synthesized in large quantity by the hydrothermal method which was used for the synthesis of C<sub>120</sub>O. From summing the area of newly observed HPLC peaks, the yield was estimated to be 2–3%. C<sub>140</sub>O can also be synthesized with Lebedkin's heating method. However, in this method, besides C<sub>140</sub>O, insoluble polymeric species were also synthesized in large quantities. From the viewpoint of recycling unreacted C<sub>70</sub>, the hydrothermal treatment was preferred over the heating method. HPLC charts and mass spectra showed the existence of polyoxides and the isomers of C<sub>140</sub>O as predicted by Fowler et al. Three isomers were isolated by HPLC and investigated by MALDI-TOF-MS, UV–Vis, FT-IR, and Raman. These results showed the similarity between C<sub>140</sub>O and C<sub>120</sub>O and support that our C<sub>140</sub>O samples have the structure of conventional furan-bridged dimer.

<sup>13</sup>C NMR measurements showed that the structure of C<sub>140</sub>O(A) was the one of isomer 1 or 2 and that the structure of C<sub>140</sub>O(B) was the one of isomer 4 or 5. Complete assignments of structures were impossible; however, we suppose that the structure of C<sub>140</sub>O(A) and (B) should be assigned to isomer 2 and 4, respectively, from Mulliken charge calculation. For C<sub>140</sub>O(C), we suppose it to have the structure of isomer 3 from the elimination method.

**Acknowledgment.** The present study was supported in part by Grant-in-Aid for Priority Research (#11165202) and International Scientific Research Program (#11694119) from the Ministry of Education, Science, Culture, and Sports of Japan and CREST of Japan Science and Technology Institute. The authors thank Mrs. Ruth Alberts for the technical support in the synthesis of C<sub>140</sub>O, Dr. Sergei Lebedkin for the advice about HPLC retention time, Dr. Jürgen Gross for the advice in MALDI measurements, Dr. Kenji Kodama and Dr. Yoko Miyake for valuable discussion about NMR measurements, and Dr. Takatoshi Matsumoto for the advice in using Mulliken charge calculations.

## References and Notes

- (1) McElvany, S. W.; Callahan, J. H.; Ross, M. M.; Lamb, L. D.; Huffman, D. R. *Science* **1993**, *260*, 1632.
- (2) Deng, J. P.; Ju, D. D.; Her, G. R.; Mou, C. Y.; Chen, C. J.; Lin, Y. Y.; Han, C. C. *J. Phys. Chem.* **1993**, *97*, 11575.
- (3) Beck, R. D.; Brauchel, G.; Stoermer, C.; Kappes, M. M. *J. Chem. Phys.* **1995**, *102*, 540.
- (4) Taylor, R. J. *Chem. Soc., Chem. Commun.* **1994**, 1629.
- (5) Lebedkin, S.; Ballenweg, S.; Gross, J.; Taylor, R.; Krätschmer, W. *Tetrahedron Lett.* **1995**, *36*, 4971.
- (6) Gromov, A.; Lebedkin, S.; Ballenweg, S.; Krätschmer, W. *Fullerenes and Fullerene Nanostructure, Proceedings of the International Winterschool on Electronic Properties of Novel Materials*; Kuzmany, H., Fink, J., Mehring, M., Roth, S., Eds.; World Scientific: Singapore, 1996; p 460.
- (7) Smith, A. B.; Tokuyama, H.; Strongin, R. M.; Furst, G. T.; Romanow, W. J. *J. Am. Chem. Soc.* **1995**, *117*, 9359.
- (8) Gromov, A.; Ballenweg, S.; Giessa, S.; Lebedkin, S.; Hull, W. E.; Krätschmer, W. *Chem. Phys. Lett.* **1997**, *267*, 460.
- (9) Kudo, T.; Takahashi, H.; Shinoda, K.; Jeyadevan, B.; Tohji, K.; Nirasawa, T.; Kasuya, A.; Nishina, Y.; Krätschmer, W. *Recent Research Developments in Physical Chemistry* **2001**, *5*, 301. Takahashi, H.; Mat-subara, E.; Kasuya, A.; Akimoto, Y.; Kudo, T.; Jeyadevan, B.; Tohji, K. *Proc. Int. Symp. on Cluster Assembled Mater. IPAP Conf.* **2001**, *3*, 118.
- (10) Deng, J. P.; Mou, C. Y.; Han, C. C. *Chem. Phys. Lett.* **1996**, *256*, 96.
- (11) Al-Jafari, M. S.; Barrow, M. P.; Taylor, R.; Drewello, T. *Int. J. Mass Spectrom.* **1999**, *184*, L1.
- (12) Wang, G. W.; Komatsu, K.; Murata, Y.; Shiro, M. *Nature* **1997**, *387*, 583.
- (13) Akimoto, Y.; Kudo, T.; Shinoda, K.; Jeyadevan, B.; Tohji, K.; Nirasawa, T.; Kasuya, A.; Nishina, Y. *Proc. Int. Symp. on Cluster Assembled Mater. IPAP Conf.* **2001**, *3*, 123.
- (14) Fowler, P. W.; Michell, D.; Taylor, R.; Seifert, G. *J. Chem. Soc., Perkin Trans. 2* **1997**, 1901.
- (15) Lebedkin, S.; Hull, W. E.; Soldatov, A.; Renker, B.; Kappes, M. M. *J. Phys. Chem. B* **2000**, *104*, 4101.
- (16) Eisler, H. J.; Hennrich, F. H.; Werner, E.; Hertwig, A.; Stoermer, C.; Kappes, M. M. *J. Phys. Chem.* **1998**, *A102*, 3889.
- (17) Adams, G. B.; Page, J. B.; Sankey, O. F.; O'Keeffe, M. *Phys. Rev.* **1994**, *B50*, 17471.
- (18) Porezag, D.; Pederson, M. R.; Frauenheim, T.; Kpöhler, T. *Phys. Rev.* **1995**, *B52*, 14963.
- (19) Krause, M.; Dunsch, L.; Seifert, G.; Fowler, P. W.; Gromov, A.; Krätschmer, W.; Gutierrez, R.; Porezag, D.; Frauenheim, T. *J. Chem. Soc. Faraday Trans.* **1998**, *94*, 2287.
- (20) Lebedkin, S.; Gromov, A.; Giesa, S.; Gleiter, R.; Renker, B.; Rietschel, H.; Krätschmer, W. *Chem. Phys. Lett.* **1998**, *285*, 210.
- (21) Bezmelnitsin, V. N.; Eletsii, A. V.; Schepetov, N. G.; Avent, A. G.; Taylor, R. J. *Chem. Soc., Perkin Trans. 2* **1997**, 683.
- (22) Balch, A. L.; Costa, D. A.; Olmsted M. M. *Chem. Commun.* **1996**, 2449.
- (23) Smith, A. B.; Strongin, R. M.; Brard, L.; Furst, G. T.; Atkins, J. H.; Romanow, W. J. *J. Org. Chem.* **1996**, *61*, 1904.
- (24) Raghavachari, K. *Chem. Phys. Lett.* **1992**, *197*, 4, 5, 495.
- (25) Wang, B. C.; Chen, L.; Chou, Y. M. *J. Mol. Struct. (THEOCHEM)* **1998**, *422*, 153.